ACS OMEGA

http://pubs.acs.org/journal/acsodf

Article

Hydrosoluble Perylene Monoimide-Based Telomerase Inhibitors with Diminished Cytotoxicity

Pak Thaichana, Ratasark Summart, Pornngarm Dejkriengkraikul, Puttinan Meepowpan, T. Randall Lee,* and Wirote Tuntiwechapikul*

Cite This: *ACS Omega* 2022, 7, 16746−16756

Read Online

ACCESS | Metrics & More | Article Recommendations | Supporting Information

ABSTRACT: Telomerase is essential for the immortality characteristics of most cancers. Telomerase-specific inhibitors should render cancer cells to replicative senescence without acute cytotoxicity. Perylene-based G-quadruplex (G4) ligands are widely studied as telomerase inhibitors. Most reported perylene-based G4 ligands are perylene diimides (PDIs), which often suffer from self-aggregation in aqueous solutions. Previously, we found that PM2, a perylene monoimide (PMI), exhibited better solubility, G4 binding affinity, and telomerase inhibition than PIPER, the prototypic PDI. However, the acute cytotoxicity of PM2 was about 20−30 times more than PIPER in cancer cells. In this report, we replaced the piperazine side chain of PM2 with ethylenediamine to yield PM3 and replaced the *N*,*N*-diethylethylenediamine side chain of PM2 with the 1-(2-aminoethyl) piperidine to yield PM5. We found that asymmetric PMIs with two basic side chains (PM2, PM3, and PM5) performed better than PIPER (the prototypic PDI), in terms of hydrosolubility, G4 binding, *in vitro* telomerase inhibition, and suppression of human telomerase reverse transcriptase (*hTERT*) expression and telomerase activity in A549 cells. However, PM5 was 7−10 times less toxic than PM2 and PM3 in three cancer cell lines. We conclude that replacing the *N*,*N*-diethylethylenediamine side chain with the 2-aminoethylpiperidine on PMIs reduces the cytotoxicity in cancer cells without impacting G4 binding and telomerase inhibition. This study paves the way for synthesizing new PMIs with drug-like properties for selective telomerase inhibition.

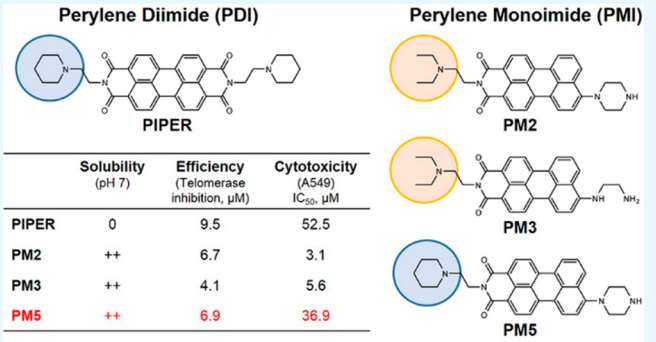

	Solubility (pH 7)	Efficiency (Telomerase inhibition, μM)	Cytotoxicity (A549) IC_{50}, μM
PIPER	0	9.5	52.5
PM2	++	6.7	3.1
PM3	++	4.1	5.6
PM5	++	6.9	36.9

INTRODUCTION

Telomerase is essential for the immortality characteristics of most cancers.[1] It allows cancer cells to maintain their telomere length, enabling them to evade replicative senescence that generally occurs in normal somatic cells.[2] Human telomerase is a ribonucleoprotein complex whose activity relies on two essential components, the human telomerase reverse transcriptase (hTERT) and the human telomerase RNA (hTR).[3] The hTERT catalytic subunit employs a section of hTR as a template to incorporate a repetitive hexameric GGTTAG sequence to the 3′-end of telomere.[4] As telomerase activity is absent in most normal somatic cells, the enzyme is an attractive target for cancer-specific therapeutics.[3]

G-quadruplex DNAs (G4s) are a group of secondary DNA structures that form from certain distinct guanine-rich sequences. G4s consist of a stack of two or more G-tetrads, which are planar ring structures assembled from Hoogsteen hydrogen bonding among four guanines.[5] This stack of G-tetrads is stabilized by ionic bonding among O_6-guanines and cations, preferably monovalent cations such as K^+ and Na^+.[5] G4 motifs are prevalent in the human genome, but studies by G4 ChIP-seq found that only a fraction of these sequences form G4 structures inside human cells.[6] These endogenous G4s are primarily found in regulatory nucleosome-depleted regions and are correlated with transcription elevation.[6] The number and location of endogenous G4s are varied on different cell types and cell states, suggesting various roles in various circumstances.[7] Many G4s are found within the promoter or the 5′-UTR of several oncogenes and tumor suppressor genes, including *MYC*, *RAS*, *MYB*, *TP53*, *JUN*, *HOXA9*, *FOXA1*, *RAC1*, *VEGF*, and *hTERT*, that are involved in numerous cancer hallmarks.[6,8] Furthermore, telomeric DNA, which consists of tandem repeats of $[TTAGGG]_n$ sequences, can form G4 DNA structures that disrupt telomere function and inhibit telomerase access.[8] Therefore, these G4 DNAs are potential therapeutic targets for cancer therapy.

Received: March 6, 2022
Accepted: April 8, 2022
Published: May 5, 2022

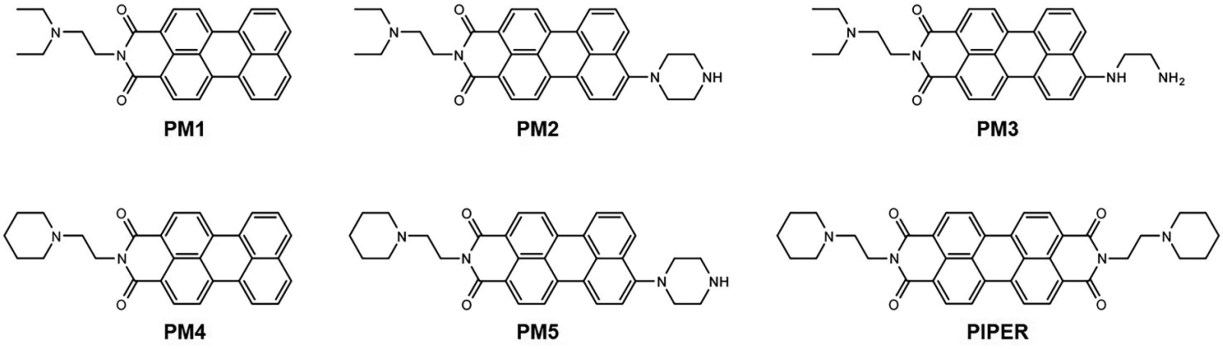

Figure 1. Chemical structures of PMIs and PIPER.

Scheme 1. Scheme Used to Synthesize the PMIs

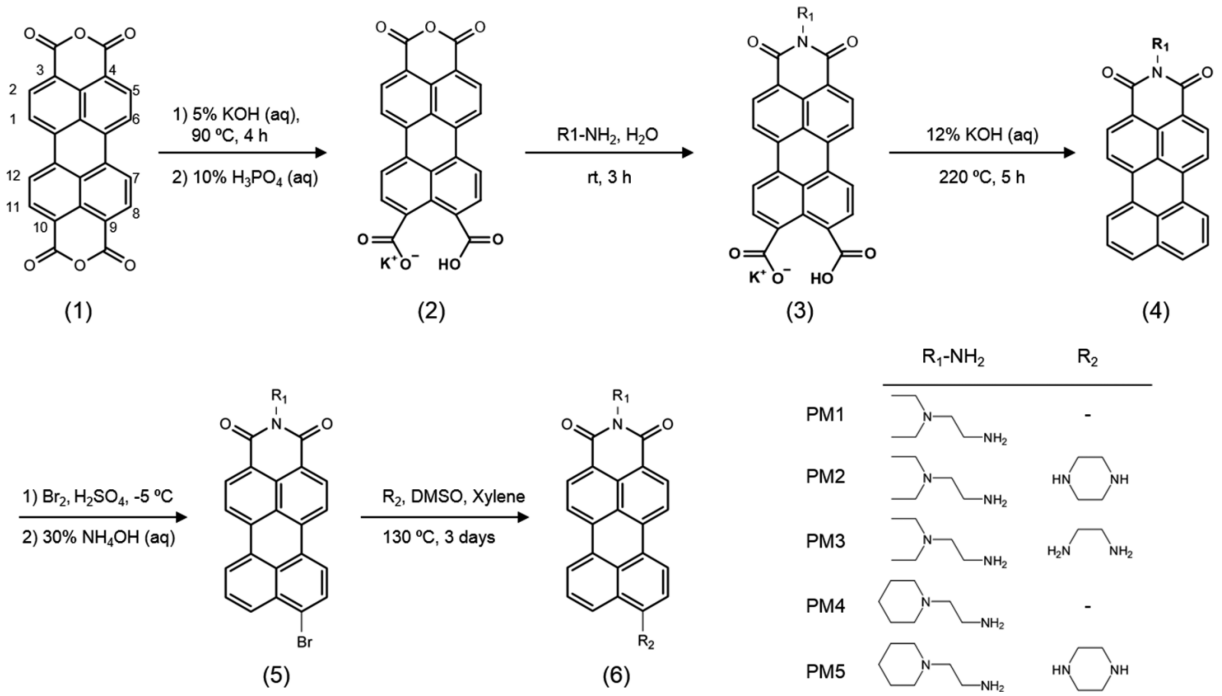

G-quadruplex ligands are small molecules that facilitate and stabilize G4 DNA formation, and they are widely studied for anticancer therapy.[9,10] G4 ligands were initially developed as telomerase inhibitors;[11,12] however, many G4 ligands have antiproliferative effects beyond telomere and telomerase.[9,10] Some G4 ligands can also interact with duplex DNA and off-targets, leading to undesirable side effects.[13,14] Telomerase inhibition by G4 ligands is well documented.[15−18] The G4 formation at the 3′-overhang of the telomere prevents telomerase from accessing its substrate, thereby inhibiting its activity.[9,11] Furthermore, G4 formation at the *hTERT* promoter suppresses *hTERT* expression and telomerase activity in cancer cells.[19,20] With these dual mechanisms, cancer cells treated with G4 ligands display gradual telomere shortening after rounds of cell division, which eventually leads to cell senescence or apoptosis.[16,20] However, some G4 ligands induce rapid replicative senescence through the displacement of shelterin proteins and telomerase uncapping, activating DNA damage response of DNA double-strand breaks.[13] For specific telomerase inhibition, prolonged time-dependent telomere attrition that leads to cellular senescence or apoptosis should be observed in cancer cells without acute cytotoxicity. Whether a G4 ligand is a specific telomerase inhibitor or acts through several mechanisms, it can probably find applications in different aspects of anticancer therapy.

In search of telomerase inhibitors, our group has been investigating perylene-based G4 ligands. Perylene is a large aromatic molecule that interacts with G4s by $\pi-\pi$ stacking on top of the outer G-tetrad.[21] While the planar system of perylene is essential for G4 binding, it also causes many perylene derivatives to be aggregated.[22] Most perylene-based telomerase inhibitors are perylene diimide derivatives derived from the prototypic perylene diimide, PIPER. PIPER induces monomeric G4s from oligonucleotides having the telomeric sequence and other G4-bearing gene promoter sequences, including *c-Myc*, *hTERT*, and *VEGF*, leading to telomerase inhibition and gene suppression, respectively.[20,23,24] In cancer cells, PIPER induces telomere shortening and subsequent cellular senescence in a prolonged time-dependent manner using only subcytotoxic doses.[20,23] However, PIPER aggregates at neutral to basic pH solution, which could affect its drug formulation.

Several strategies have been developed to increase the solubility of perylene diimides, including modification of the

https://doi.org/10.1021/acsomega.2c01343
ACS Omega 2022, 7, 16746−16756

side chains,[22,25,26] bay area,[27] and recently, asymmetric PDI.[28] Previously, we found that PM2, a perylene monoimide (PMI) derivative, exhibited better solubility, G4 binding affinity, and telomerase inhibition than PIPER.[20,23] Both PM2 and PIPER inhibited telomerase and induced telomere shortening and cellular senescence in lung and prostate cancer cells.[20,23] However, the acute cytotoxicity of PM2 was about 20−30 times more than that of PIPER in cancer cells, while the cellular uptake of both compounds was comparable.[20,23] We hypothesized that PM2 induced cytotoxicity in cancer cells via other mechanisms besides telomerase inhibition and wondered whether one or both side chains of PM2, or PMI in general, were responsible for the increase in its toxicity. Therefore, in this report, we replaced the piperazine side chain of PM2 with the ethylenediamine, to yield PM3, and replaced the *N*,*N*-diethylethylenediamine side chain of PM2 with the 1-(2-aminoethyl) piperidine side chain of PIPER, to yield PM5. We found that the acute cytotoxicity of PMIs with *N*,*N*-diethylethylenediamine side chain (PM1-PM3) is 7−10 times more than the PMIs with 1-(2-aminoethyl) piperidine side chain (PM4 and PM5) in three different cancer cell lines, while the G4 binding, *hTERT* suppression, and telomerase inhibition are comparable to PM2. These PMIs are also more soluble than PIPER and have a range of colors that could be useful as fluorescent probes for environmental and biological analysis.[29,30] The structure of these PMIs and PIPER are shown in Figure 1.

RESULTS AND DISCUSSION

Syntheses of Perylene Monoimide Derivatives (PMIs). The syntheses of the PMIs (PM1-PM5) followed the synthetic strategy of PM1 and PM2 described by Huang.[31,32] The general procedure of the syntheses is demonstrated in Scheme 1. First, one of the two anhydride rings of perylene-3,4,9,10-tetracarboxylic dianhydride (PTCDA, 1) is opened in a two-step reaction. The steps involve hydrolyzation of both anhydride rings by 5% KOH in water at 90 °C for 4 h, and then one anhydride ring is reformed by dropwise addition of 10% H_3PO_4 until the pH is between 4.5 and 5.5 to give the intermediate (2). The monopotassium salt of (2) is then refluxed with the primary amine of R_1 in water at room temperature for 3 h to attach the side chain at the anhydride ring to give (3). Decarboxylation of (3) in 12% KOH at 220 °C in a closed steel vessel produces perylene monoimide (4). If the R_1-NH_2 side chain is *N*,*N*-diethylethylenediamine, the product (4) is PM1; if it is 1-(2-aminoethyl) piperidine, the product (4) is PM4. Bromination of compound (4) using Br_2 and sulfuric acid at −5 °C, followed by neutralization with 30% NH_4OH, gives the intermediate (5). Substituting Br in (5) by piperazine or ethylenediamine yields the corresponding PMIs (PM2, PM3, and PM5), depending on their side chains. The detailed syntheses and characterization data of these compounds are described in Supporting Information S1 and Figures S1−S6.

While PDIs can be synthesized in one step from perylene-3,4,9,10-tetracarboxylic dianhydride, the synthesis of PMIs involves several steps of selective addition of the asymmetric side chains. This difficulty might discourage researchers from synthesizing new PMIs, but there are several advantages of making asymmetric PMIs. Since perylene derivatives have many science and modern technology applications,[29,30,33−35] the two different side chains of PMIs offer a broader range of physical, chemical, and biological properties than symmetric PDIs. Researchers can also select a particular side chain to suit their desired purpose. As demonstrated in our previous publication, aPDI−PHis, an asymmetric perylene diimide derivative with a 2-aminoethylpiperidine side chain and a histidine side chain, is superior to its symmetric counterparts in terms of hydrosolubility, G4 binding, cellular uptake, and telomerase inhibition in prostate cancer cells.[28]

Hydrosolubility of PMIs and PIPER. Perylene diimide derivatives (PDIs) with basic side chains often aggregate at neutral to basic pH. To test whether our PMIs could solubilize in an aqueous solution at physiological pHs, a 40 μM solution of each PMI or PIPER was prepared in a plastic cuvette using 10 mM buffer pH 5 to pH 9, and the solutions were observed at various times up to 7 days. As expected from their structures, these compounds completely precipitated after 48 h at basic pH 8 and 9, where their side chains were not protonated, and they were soluble at acidic pH 5 and 6, where their side chains were protonated (Supporting Information Figure S7A). At pH 7, PIPER started to aggregate after 12 h and completely precipitated within 2 days, while other PMIs remained soluble at this pH throughout 7 days (Supporting Information Figure S7). The ability of PMIs to be soluble at neutral pH is an advantage over PIPER from a pharmaceutical perspective.

Hydrosolubility of perylene derivatives has been a subject of improvement ever since the discovery of PIPER as a G4 ligand.[21,22] Self-aggregation of PDIs is a constant problem due to the large planar system of the perylene core. However, this same perylene core is also essential for the $\pi-\pi$ stacking to the outer G-tetrad of G4 DNA. Studies showed that ligand aggregation correlated with the G4 binding and selectivity.[36,37] Therefore, there is a delicate balance between the G4 binding and the hydrosolubility; too soluble in aqueous solution results in less selective G4 binding and ineffective biological activities. The compound should remain soluble until it reaches the target cells and becomes less soluble inside the nucleus where the targeted G4 DNAs are. Modifications of one or both side chains of PDIs are often limited to positively charged side chain, where it interacts with the G4 groove. The pH-dependent positive charge of the nitrogen-containing side chain seems to serve this purpose well because the perylene derivatives are less soluble in neutral to basic pH, which is the pH inside the cell. This study demonstrates that the PMIs aggregate less than PIPER at pH 7. It is likely because the asymmetric nature of these molecules may slightly twist the aromatic plane of the perylene core that prevents aggregation at this pH. However, these PMIs still aggregate at the basic pHs, which may aid the G4 binding in the cell.

On the other hand, the solubility of hydrophobic drugs could also be solved with various drug delivery systems.[38] For example, halloysite-based nanoformulations and polyelectrolyte nanocapsules have successfully delivered hydrophobic anticancer drugs to several cancer cell lines.[39,40] However, drug delivery into the target cells alone might be insufficiently effective for drugs that target specific DNA structures inside the cells, as in our case, the G4 structures. Drug aggregation inside the cells can still diminish its effectiveness. Furthermore, binding to specific G4 structures, among various forms of G4s, is also essential for G4-based telomerase inhibitors. We previously found that PM2 and aPDI−PHis suppressed telomerase activity and *hTERT* expression at lower concentrations than PIPER, despite the comparable cellular uptake.[23,28] Therefore, we opted to modify our perylene

https://doi.org/10.1021/acsomega.2c01343
ACS Omega 2022, 7, 16746−16756

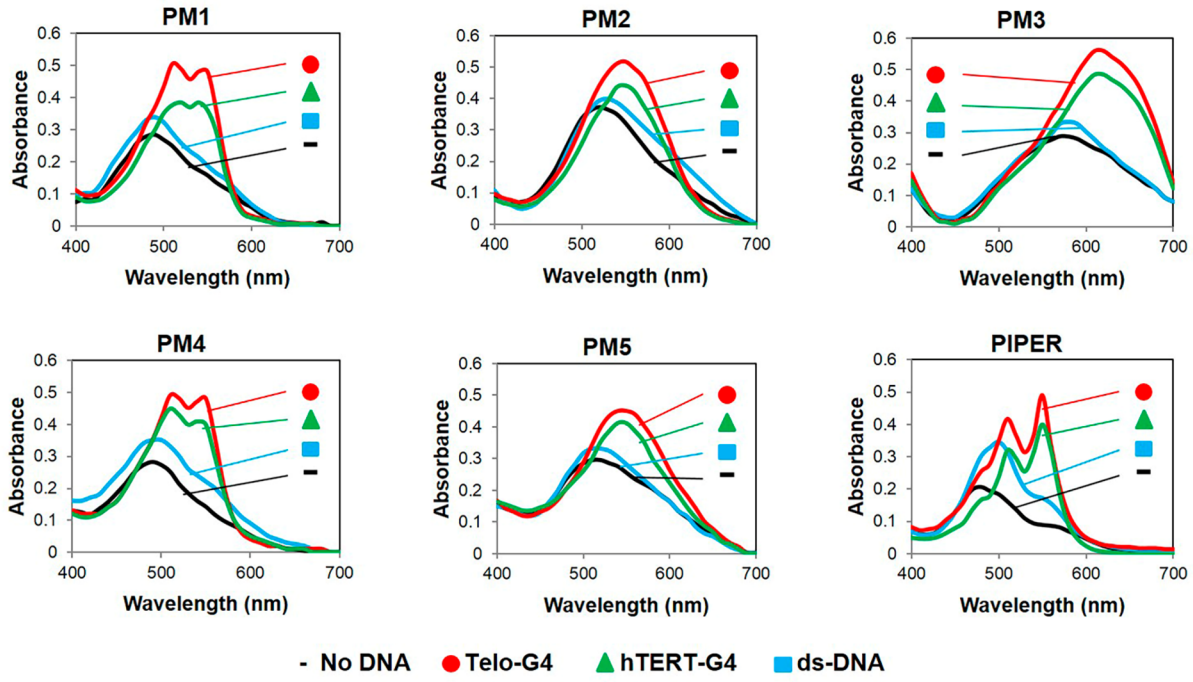

Figure 2. DNA binding of PMIs and PIPER by spectrophotometry. The indicated perylene derivative (40 μM) was incubated in the absence and presence of the indicated preformed DNA (20 μM) in 10 mM potassium phosphate buffer (pH 7.4) supplemented with 100 mM KCl for 24 h before the visible light absorption spectra were recorded by a spectrophotometer. The preformed DNAs were two G4 DNAs from the telomeric sequence (Telo-G4), the *hTERT* promoter sequence (hTERT-G4), and a double-stranded DNA (ds-DNA) from a 12-mer self-annealed sequence.

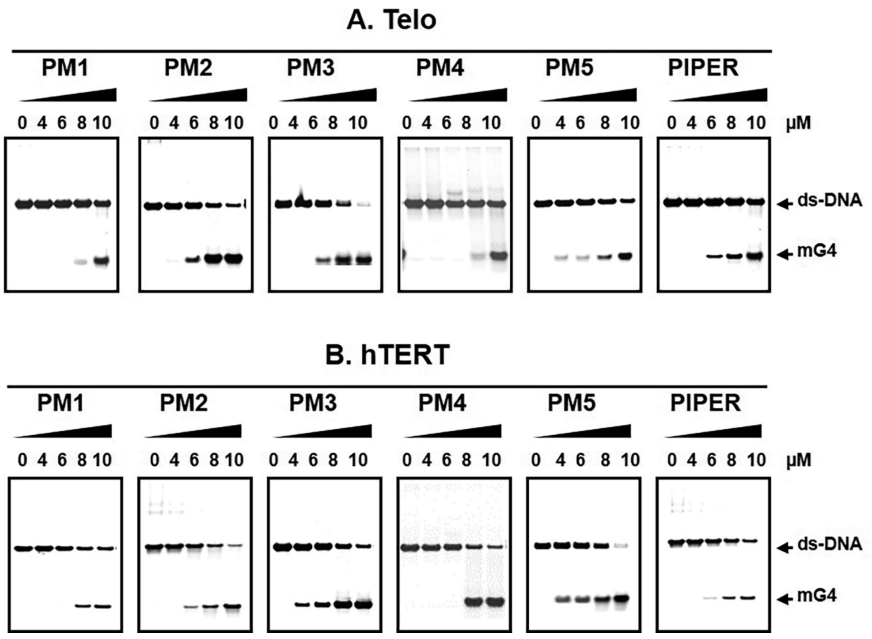

Figure 3. G-quadruplex binding selectivity of PMIs and PIPER by duplex−quadruplex competition assay using telomeric sequence (A) and the *hTERT* promoter sequence (B). The 20 μL reaction mixture, consisting of the fluorescence-labeled G4 strand (2 μM), its complementary C-rich strand (2 μM), and the indicated concentration of a perylene derivative (0−10 μM) in 10 mM potassium phosphate buffer (pH 7.4) containing 100 mM KCl, was first denatured at 95 °C for 5 min and then incubated at 55 °C for 10 h in a thermocycler before cooling to 4 °C. The samples were separated by electrophoresis at 4 °C in a 16% nondenaturing polyacrylamide gel. Bands are identified as ligand-bound monomeric G-quadruplex (mG4) and duplex (ds-DNA).

chemically to solve the hydrosolubility issue and improve G4 binding to our targeted G4 structures.

The colors of these PMIs cover a wide range, from orange, orange-red, purple, dark purple, to blue. The visible light absorption and fluorescence emission spectra of these PMIs are supplied in Supporting Information Figure S8. Since perylene derivatives have strong fluorescence emission and high photostability, these hydrosoluble PMIs could be useful as fluorescent probes for cell and organelle imaging, as well as fluorescent tools for environmental and biological analysis.[41,42]

https://doi.org/10.1021/acsomega.2c01343
ACS Omega 2022, 7, 16746−16756

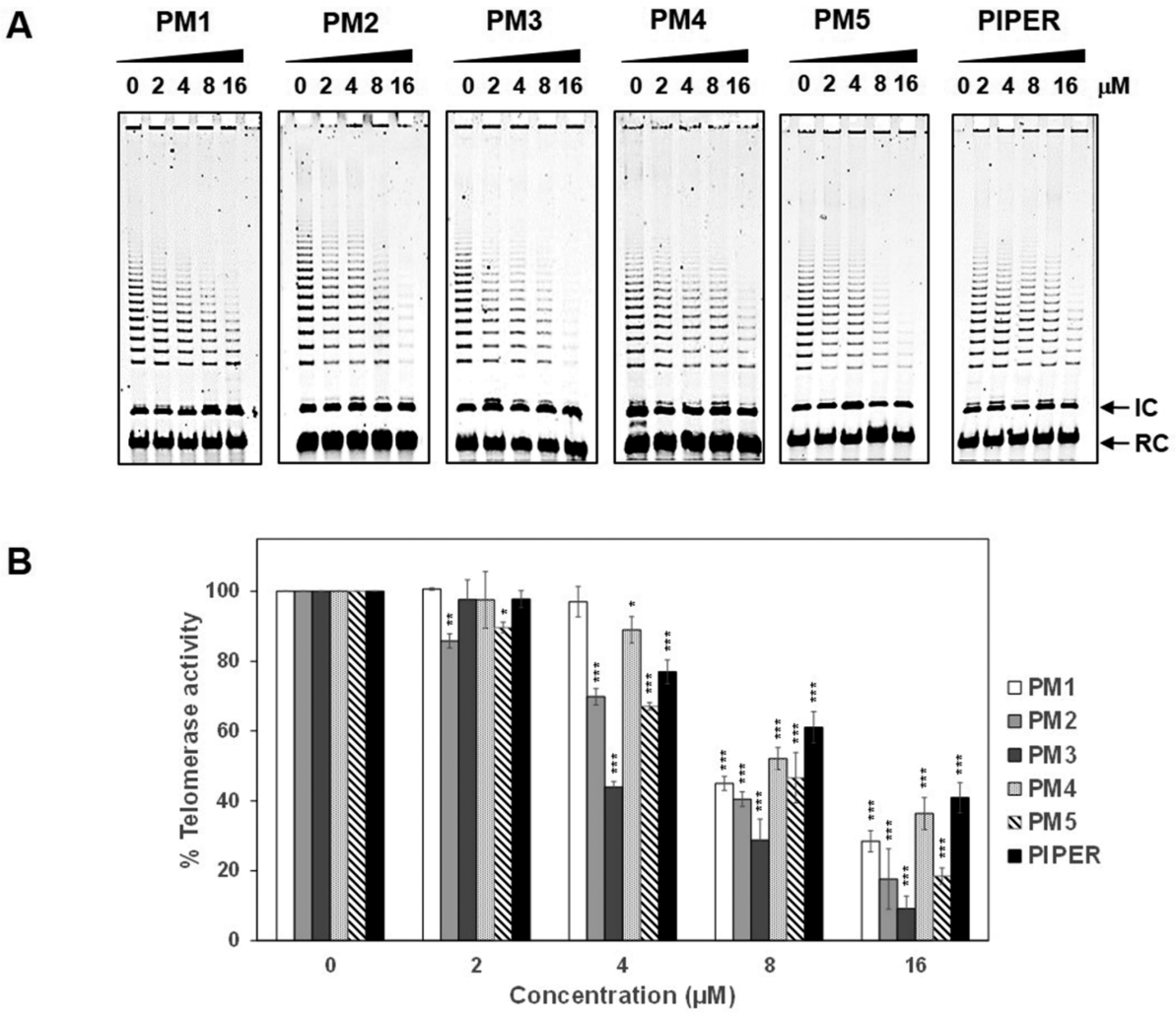

Figure 4. Telomerase inhibition of PMIs and PIPER in a cell-free system by modified TRAP assay. (A) Telomerase inhibition assay, TSG4 primer was first incubated with the indicated concentration of a PMI or PIPER at 37 °C for 2 h in a telomerase reaction mixture (pH 7.4). The crude telomerase extract was then added to the mixture, and the telomerase extension reaction was allowed at 30 °C for 30 min. The perylene was removed by phenol-chloroform extraction, and the telomerase products were amplified by PCR. The amplified products were separated by nondenaturing polyacrylamide gel electrophoresis, and the images were captured using a phosphoimager. IC is the internal control, and RC is the recovery control. (B) Bar graphs illustrate the quantitative results from the telomerase inhibition assay. Each bar represents the mean ± SD from three independent experiments. Statistical significance is defined as (*) $p < 0.05$, (**) $p < 0.01$, and (***) $p < 0.001$.

G4 DNA Binding Study by Spectrophotometry. Telomerase activity in cancer cells can be suppressed through G-quadruplex formations at the *hTERT* promoter and the 3′-overhang of the telomere. To test whether our PMIs could bind to these G4 DNAs, we employed spectrophotometry to study the DNA binding at cellular pH and potassium ion concentration. Each PMI or PIPER (40 μM) was dispersed in 10 mM potassium phosphate buffer (pH 7.4) containing 100 mM KCl in the absence or presence of a preformed DNA structure (20 μM) for 24 h at room temperature. The DNA structures investigated were two G4 DNAs from the telomeric sequence (Telo-G4) and the *hTERT* promoter sequence (hTERT-G4), and a double-stranded DNA (ds-DNA) from a 12-mer self-annealed sequence. The visible absorption spectra between 400 and 700 nm were recorded after 24 h incubation. As shown in Figure 2, these PMIs and PIPER started to aggregate at pH 7.4 after 24 h incubation without DNA. However, there was an increase in light absorption and a spectral shift in the presence of a DNA structure, which indicates DNA binding. In general, the PMIs and PIPER appeared to bind preferentially with the Telo-G4 DNA, followed by hTERT-G4 DNA and ds-DNA, respectively.

G4 DNA Binding Selectivity Study by Duplex–Quadruplex Competition Assay. Therapeutic G4 ligands should bind selectively to their respective G4 DNA targets because nonspecific binding to duplex DNA generally leads to cellular toxicity.[13] The G4 binding selectivity of our PMIs and PIPER was further determined using a duplex–quadruplex competition assay. The assay was performed in a mixture of a fluorescence-labeled G4 strand and its complementary strand, under conditions where these two strands form a duplex. If a test compound is preferentially bound to the G4-DNA, it induces G4 formation. The monomeric G4 (mG4) or tetrameric G4 (tG4) appeared below or above the duplex band (ds-DNA), respectively, while the duplex band disappears with increasing amounts of the test compound. On the other hand, if a test compound preferentially binds to a duplex DNA, the G4 band is not present, and the duplex band is thicker with the increased amount of the test compound.[26]

https://doi.org/10.1021/acsomega.2c01343
ACS Omega 2022, 7, 16746−16756

We performed this assay using the same G4 sequences, the telomeric sequence (Figure 3A, Telo) and the *hTERT* promoter sequence (Figure 3B, hTERT). As observed in Figure 3A and 3B, without a test compound (Lane 0) both G4 sequences formed duplex DNA (ds-DNA) with their complementary strands. In the presence of a PMI or PIPER, the mG4 band increased, while the ds-DNA band decreased in a concentration-dependent manner. These results show that the PMIs and PIPER preferentially bind and stabilize monomeric G4, not duplex DNA. PMIs with only one side chain on the imide-side (PM1 and PM4) are the least effective G4 binder among all perylene derivatives. The PMIs with two side chains (PM2, PM3, and PM5) appeared to induce mG4 at a lower concentration than PIPER.

Both spectrophotometry and duplex−quadruplex competition assays showed that all PMIs and PIPER preferentially bound both G4 DNAs to duplex DNA. Regarding G4 DNA binding affinity, the PMIs with two basic side chains (PM2, PM3, and PM5) bound G4 DNAs better than PIPER, while PMIs with one basic side chain (PM1 and PM4) bound G4 DNAs less than PIPER.

In general, G4 ligands with polycyclic aromatic cores bind to G4 DNAs via $\pi-\pi$ stacking on the outer G-tetrad.[43] The basic side chains interact with phosphate groups in the G4 grooves, likely through bridging with the water network inside the grooves rather than direct contact.[43] For perylene-based G4 ligands, NMR studies found that PIPER and perylene-EDTA also stacked on the terminal G-tetrad.[44,45] Notably, the loops around the G4 structure might contribute to the selectivity of ligand binding; this is not well understood, and it needs more structural data to deduce any rational drug design.[43] Our preliminary data based on molecular modeling show the predicted mode of G4 binding and estimate the binding affinity of our PMIs and PIPER to two G4 structures (Telomeric G4 and hTERT G4) as described in the Supporting Information (see Figure S9 and Table S1). The molecular docking data support the results from our spectrophotometry and duplex−quadruplex competition assays of which PMIs with two basic side chains (PM2, PM3, and PM5) exhibit higher binding affinity than PMIs with one basic side chain (PM1 and PM4).

Telomerase Inhibition in a Cell-Free System. G4 ligands facilitate G4 formation at the 3′-overhang of telomeric DNA, preventing telomerase from accessing its substrate, thereby inhibiting its activity. In this experiment, we employed our modified TRAP assay to assess the ability of our new PMIs to inhibit telomerase.[20,23,28] The TSG4 primer was first incubated with various concentrations of a test compound for 2 h at 37 °C to allow G4 formation before the telomerase reaction mixture was added. After the telomerase extension reaction, the test compound was extracted from the reaction mixture by phenol/chloroform extraction, and telomerase products were precipitated by ethanol. The precipitants were resuspended in a PCR reaction mixture to amplify the telomerase products, and these products were then separated by nondenaturing PAGE. As shown in Figure 4A, all PMIs and PIPER inhibited telomerase in a concentration-dependent manner. The amplified telomerase products from three separate experiments were then quantified, and the percentage telomerase activity was plotted against the compound concentration (Figure 4B). The half-maximal inhibitory concentrations (IC_{50}) of all test compounds were calculated from the graph and are summarized in Table 1. The efficacy of telomerase inhibition by these compounds is in the following order: PM3 (4.1 ± 0.5 μM) > PM2 (6.7 ± 0.3 μM) ≈ PM5 (6.9 ± 0.2 μM) > PM1 (7.6 ± 0.1 μM) > PM4 (8.6 ± 0.6 μM) > PIPER (9.5 ± 0.8 μM). It appears that all perylene derivatives inhibit telomerase with the PMIs (PM1−PM5) being slightly more effective than the PDI, PIPER. The PMIs having two side chains (PM2, PM3, and PM5), which bind G4 better than the PMIs with one side chain (PM1 and PM4), appear to be more effective telomerase inhibitors as well.

Table 1. IC_{50} Values of PMIs and PIPER on *In Vitro* Telomerase Inhibition

compound	telomerase inhibition (μM)
PM1	7.6 ± 0.1
PM2	6.7 ± 0.3
PM3	4.1 ± 0.5
PM4	8.6 ± 0.6
PM5	6.9 ± 0.2
PIPER	9.5 ± 0.8

Acute Cytotoxicity Assay. Specific telomerase inhibitors should selectively target telomerase without affecting cell viability. Previously, we found that PM2 is about 20−30 folds more toxic than PIPER to A549 lung cancer cells and PC3 prostate cancer cells.[20,23] In this experiment, we investigated whether side chain modification of PMI could affect their cytotoxicity. We employed the standard sulforhodamine B (SRB) assay to evaluate the acute cytotoxicity in three different human cancer cell lines (A549 nonsmall cell lung carcinoma, PC3 prostate adenocarcinoma, and HL60 promyelocytic leukemia), along with HEK293 human embryonic kidney cells and peripheral blood mononuclear cells (PBMC). These cells were treated with various concentrations of a test compound for 72 h before the cell viability was evaluated. The half-maximal inhibitory concentrations (IC_{50}) of all perylene derivatives, including doxorubicin as an assay control, were calculated and are summarized in Table 2. The IC_{50} values of doxorubicin in these cells are comparable to previous studies [see Supporting Information Table S2].

As shown in Table 2, all perylene derivatives were much more toxic to the three cancer cell lines (A549, PC3, and HL60) than the noncancerous cell line HEK293 and the peripheral blood mononuclear cells (PBMC), in contrast to doxorubicin, which affected all five cell types similarly. These results are encouraging for perylenes to be used as selective anticancer agents. Among the three cancer cell lines, the IC_{50} values from each perylene derivative are not much different; therefore, we discuss them as a group below. Among the PMIs, the IC_{50} values from PM1, PM2, and PM3 are between 3.1 and 7.4 μM, while the IC_{50} values from PM4 and PM5 are between 36.9 and 50.9 μM. The IC_{50} values from PM4 and PM5 are closer to PIPER, which is between 52.5 and 86.2 μM in the three cancer cell lines. These results are consistent with our previous findings that PM2 is 20−30 times more toxic than PIPER in A549 and PC3 cancer cells.[20,23] As we mentioned earlier, PM1, PM2, and PM3 have an *N*,*N*-diethylethylenediamine side chain, while PM4, PM5, and PIPER have a 2-aminoethylpiperidine side chain. The change had little effect on the G4 binding and the telomerase inhibition, but it greatly affected the acute cytotoxicity of these compounds in cancer cells. We believe that the *N*,*N*-diethylethylenediamine side chain contributes to the cytotoxicity effect of PMIs via a different mechanism(s) rather than G4 binding.

https://doi.org/10.1021/acsomega.2c01343
ACS Omega 2022, 7, 16746−16756

Table 2. IC_{50} Values of PMIs and PIPER on Cell Viability

	cell type (μM)				
compound	A549	PC3	HL60	HEK293	PBMC
PM1	4.1 ± 0.9	5.1 ± 0.8	5.5 ± 1.2	190.93 ± 13.3	204.2 ± 18.4
PM2	3.1 ± 1.5	4.0 ± 2.3	4.8 ± 1.7	197.23 ± 17.5	212.6 ± 15.7
PM3	5.6 ± 0.8	7.0 ± 1.3	7.4 ± 1.2	204.30 ± 18.0	235.4 ± 19.1
PM4	38.4 ± 1.5	40.1 ± 4.6	43.4 ± 6.0	246.94 ± 12.6	280.4 ± 16.9
PM5	36.9 ± 4.0	42.9 ± 5.2	50.9 ± 5.9	257.98 ± 13.8	291.8 ± 18.2
PIPER	52.5 ± 5.8	84.6 ± 6.1	86.2 ± 9.4	278.01 ± 15.5	318.2 ± 19.5
Doxorubicin	1.8 ± 0.9	2.7 ± 1.3	0.07 ± 0.04	4.8 ± 2.0	5.2 ± 1.8

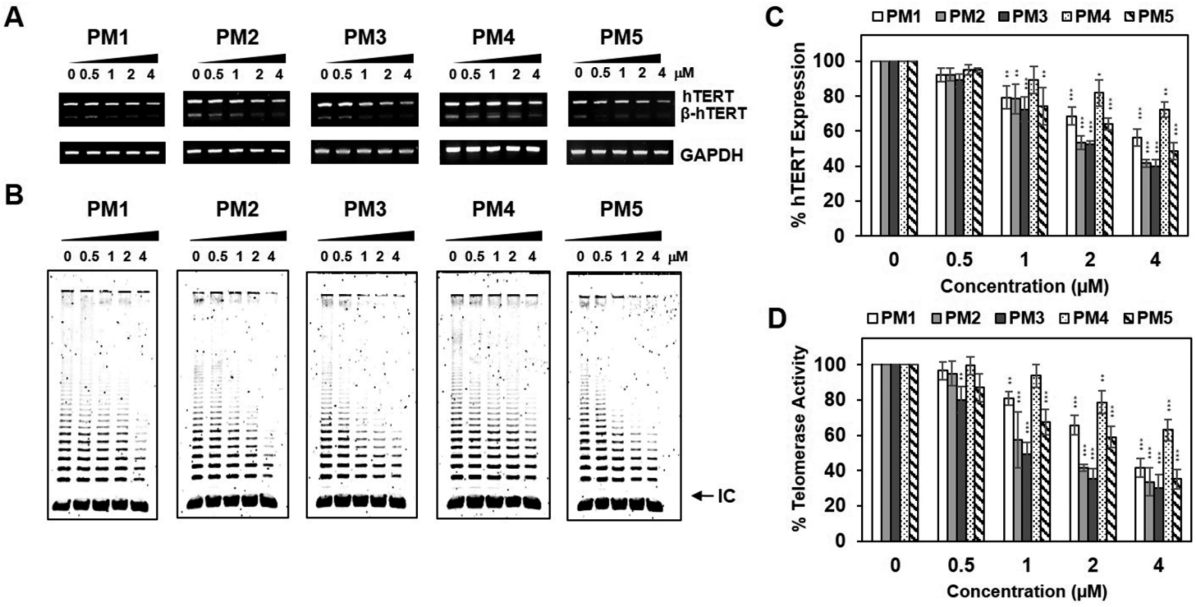

Figure 5. Suppression of *hTERT* expression (A,C) and telomerase activity (B,D) by the PMIs in A549 lung cancer cells. (A) Assay for *hTERT* expression, A549 cells were incubated with the indicated concentrations of PMIs for 24 h before their RNAs were extracted and analyzed by semiquantitative RT-PCR. (B) Assay for telomerase activity, A549 cells were incubated with the indicated concentrations of PMIs for 48 h before the crude protein extract was used as the source of telomerase in our modified TRAP assay. (C,D) The quantitative results from the *hTERT* expression and the telomerase activity assays are illustrated by bar graphs. Each bar represents the mean ± SD from three independent experiments. Statistical significance is defined as (*) $p < 0.05$, (**) $p < 0.01$, and (***) $p < 0.001$.

Suppression of *hTERT* Expression and Telomerase Activity by PMIs and PIPER in A549 Lung Cancer Cells. The *hTERT* core promoter contains several G-motifs that can form G4s,[19,46] and G4 induction by G4 ligands can mitigate telomerase activity in cancer cells via suppressing *hTERT* expression at the transcriptional level.[20,47] We previously showed that one G4 motif at the *hTERT* core promoter could be induced by PM2 and PIPER, and these compounds suppressed *hTERT* expression and telomerase activity.[20] In this experiment, we assessed the ability of PMIs in suppressing *hTERT* expression and telomerase activity in the A549 lung cancer cells using a semiquantitative RT-PCR assay and our modified TRAP assay, respectively. On the basis of our previous publications,[20,23] PM2 suppressed *hTERT* expression and telomerase activity at a lower concentration than PIPER. To compare the five PMIs, we chose the same doses between 0 and 4 μM to treat the A549 cells, while the doses for PIPER were between 0 and 16 μM (see Supporting Information Figure S10A). For the RT-PCR assay, the A549 cells were incubated with a test compound for 24 h before mRNAs extraction, cDNAs conversion, and PCR amplification by gene-specific primers. The number of PCR cycles used for each gene was carefully chosen so that the results reflected the number of the original cDNAs. Figure 5A shows the gel data from the RT-PCR experiments, and the bar graphs in Figure 5C summarize the relative *hTERT* expression quantified from the gel data. As shown in Figure 5A, the PMIs could suppress *hTERT* expression in a concentration-dependent manner. Among the five PMIs, the efficacy of *hTERT* suppression by these compounds is in the following order: PM3 > PM2 > PM5 > PM1 > PM4 (Figure 5C).

For the telomerase assay, the A549 cells were incubated with the same concentrations of PMIs and PIPER as in the RT-PCR experiments for 48 h before the crude proteins were extracted to use as the telomerase source in our modified TRAP assay. Figure 5B shows the gel data from the TRAP assay, and the bar graphs in Figure 5D summarize the percentage telomerase activity quantified from the gel data to compare the efficacy of the PMIs. The results from PIPER are shown in Supporting Information Figure S10B. As shown in Figure 5B, the PMIs suppress telomerase activity in a concentration-dependent manner. In comparison among the five PMIs (Figure 5D), the suppression of telomerase activity increases in the following order: PM3 > PM2 > PM5 > PM1 > PM4. The results from both experiments are consistent with the above G4 binding study in which the stronger G4 binders (PM3, PM2, and PM5)

https://doi.org/10.1021/acsomega.2c01343
ACS Omega 2022, 7, 16746−16756

suppress *hTERT* expression and telomerase activity more than the weaker G4 binders (PM1 and PM4).

Altogether, PMIs with two side chains (PM2, PM3, and PM5) started to induce G4 formation at a lower concentration than PIPER, while PMIs with one side chain (PM1 and PM4) started to induce G4 formation at a higher concentration than PIPER. When the A549 cells were treated with these compounds, the *hTERT* RNA expression was suppressed in a concentration-dependent manner. PIPER appeared to be the least effective among these perylene derivatives. Among the PMIs, those with two side chains (PM2, PM3, and PM5) suppressed *hTERT* expression better than those with one side chain (PM1 and PM4). The suppression of *hTERT* expression by PM1 was much more effective than PM4 despite their minimal difference in G4 binding. This discrepancy could arise from other mechanisms that affect cell viability, considering that PM1 is almost 10 times more toxic than PM4 in A549 cells. PM2 and PM3 were also more toxic than PM5 (11.9 times for PM2 and 6.6 times for PM3), and their *hTERT* suppression appeared to be slightly better than PM5. The suppression of *hTERT* expression correlates well with the telomerase activity of the crude telomerase extract from the A549 cells treated with these compounds, which followed the same trend as in the *hTERT* expression assay.

Specific telomerase inhibitors should work directly against telomerase by inhibiting its activity or production. The ultimate effect of telomerase inhibition should then lead to telomere shortening in cancer cells without affecting cell growth and cell viability. Once one or a few telomeres are shortened to a critical length, cancer cells enter cellular senescence or apoptosis.[48] G4 ligands can inhibit telomerase by inducing G4 structures at the 3′-overhang of the telomere and the *hTERT* promoter, suppressing both telomerase activity and telomerase production. However, G4 ligands can potentially facilitate G4 formation on numerous sites within the genome or bind to double-stranded DNA, leading to nonspecific cytotoxicity. For example, Telomestatin and BRACO-19, well-known G4 ligands and telomerase inhibitors, had the IC_{50} against various cancer cells between 0.5 and 4.1 μM and 1.45 and 10.6 μM, respectively.[49−55] These two compounds were found to affect cancer cells beyond telomerase inhibition.[49,55] It is unlikely to find a G4 ligand that specifically inhibits telomerase, but such an agent could be useful in scientific research and cancer therapy.

In conclusion, we demonstrate that asymmetric PMIs with two basic side chains perform better than the prototypic PDI, PIPER (in terms of hydrosolubility), G4 binding (*in vitro* telomerase inhibition), and suppression of *hTERT* expression and telomerase activity in A549 cells. All PMIs and PIPER are selectively more toxic to cancer cells than noncancerous cells. Replacing the *N*,*N*-diethylethylenediamine side chain with the 2-aminoethylpiperidine on PMIs significantly reduces the cytotoxicity in cancer cells without impacting G4 binding and telomerase inhibition, which makes PM5 a less toxic telomerase inhibitor than PM2 and PM3. This study offers viable strategies for synthesizing new PMIs with drug-like properties for selective telomerase inhibition.

METHODS

Materials. Molecular grade chemicals were purchased from commercial suppliers. Oligonucleotides and FAM-tagged oligonucleotides were supplied by Bio Basic (Canada). PIPER, which was synthesized and reported in our previous publication,[28] was used in this study as a control.

Synthesis of Perylene Monoimides. Scheme 1 and the associated text summarize the syntheses of the PMIs; additional experimental details and characterization data are provided in the Supporting Information (see Schemes S1−S3 and Figures S1−S5). We employed a Bruker NEO 400 MHz spectrometer to record the ^{1}H NMR spectra, In addition, we used a Thermo LTQ XL instrument to collect the mass spectra, and a Gallenkamp Electrothermal apparatus to measure the melting points.

Hydrosolubility Test. A 40 μM solution of each PMI or PIPER was prepared in a microcentrifuge tube using 10 mM buffer (pH 5 to pH 9) and transferred to a plastic cuvette. We observed and recorded the solubility and aggregation of the solution by a scanner periodically for up to 7 days. A UV-1800 spectrophotometer (Shimadzu Scientific) and a Synergy H4 microplate reader (BioTek Instruments, Inc.) were employed to obtain visible-light absorption spectra and fluorescence emission spectra.

Analysis of DNA Binding by Spectrophotometry. We mixed a specified preformed aliquot of DNA (20 μM) with each perylene derivative (40 μM) in 500 μL of 10 mM potassium phosphate buffer (pH 7.4) supplemented with 100 mM KCl before the visible absorption spectra between 400 and 700 nm were recorded at the indicated times using the UV-1800 spectrophotometer (Shimadzu Scientific). The sequences of oligonucleotides used in this assay can be found in Supporting Information Table S3.

Duplex−Quadruplex Competition Assay. We first mixed a 20 μL solution containing a FAM-tagged G-rich strand (2 μM), its complementary C-rich strand (2 μM), a test compound at the indicated concentration, 100 mM KCl, and 10 mM potassium phosphate buffer (pH 7.4). The mixture was then heated at 95 °C for 5 min before being incubated at 55 °C for 10 h in a thermocycler. We separated the DNA structures using 16% nondenaturing polyacrylamide gel electrophoresis at 4 °C with both electrophoresis buffer and gel supplemented with 50 mM KCl. A phosphoimaging system (Typhoon; Molecular Dynamics) visualized and recorded the separated duplex (DS) and the ligand-bound monomeric G-quadruplex (mG4) from the gel. The sequences of oligonucleotides used in this experiment are shown in Supporting Information Table S4.

Telomerase Assay in a Cell-Free System. We assessed the telomerase inhibitory effect of PMIs in a cell-free system using our fluorescence-based TRAP assay.[28] A test compound was first incubated in a 90 μL mixture containing 15 pmol TSG4 primer, 200 μM dNTPs, 20 mM Tris−HCl (pH 7.4), 63 mM KCl, 1.5 mM $MgCl_2$, 1 mM EGTA, 0.005% Tween 20, and 0.1 mg/mL bovine serum albumin at 37 °C for 2 h. Then, crude telomerase extract (10 μL, 500 ng) was added. The telomerase extension reaction was allowed for 30 min at 30 °C before it was terminated by heating at 95 °C for 5 min. We removed the test compound by phenol-chloroform extraction before telomerase products were amplified by PCR, using a 100 nM FAM-tagged RC duplex as the recovery control. The purified telomerase products (5 μL) were then added to a reaction mixture (45 μL) containing 0.25 pmol RPc3g, 15 pmol RP-FAM, 0.01 pmol IC, 7.5 pmol NT, 2.5 units Taq DNA polymerase, 200 μM dNTPs, 20 mM Tris−HCl (pH 7.4), 63 mM KCl, 1.5 mM $MgCl_2$, 1 mM EGTA, 0.1 mg/mL bovine serum albumin, and 0.005% Tween 20. PCR was

https://doi.org/10.1021/acsomega.2c01343
ACS Omega 2022, 7, 16746−16756

performed as described previously.[28] The amplified telomerase products were then separated by nondenaturing polyacrylamide gel electrophoresis. We visualized and quantified the products with a phosphoimaging system (Typhoon; Molecular Dynamics) and ImageJ software. The assay was performed in three independent experiments, and the $IC_{50} \pm SD$ values for telomerase inhibition were calculated. Supporting Information Table S5 summarized the oligonucleotides used in this assay.

Cell Culture. We obtained human cancer cell lines (A549, PC3, and HL60) and HEK293 from the American Type Culture Collection (ATCC, Rockville, MD). The peripheral blood mononuclear cells (PBMC) were collected from healthy volunteers. We cultured all cells in Roswell Park Memorial Institute medium 1640 (RPMI 1640) with 1% antibiotics (50 μg/mL streptomycin, 50 units/ml penicillin) and 10% fetal bovine serum (FBS) at 37 °C in a cell culture incubator having humidified air with 5% CO_2.

Cell Growth Inhibition Assay. The cell growth inhibition of the perylene derivatives was determined using the standard sulforhodamine B (SRB) assay.[56] The cancer cells (1.0×10^4 cells), HEK293 cells (1.0×10^4 cells), or PBMC cells (1.0×10^5 cells) were incubated with various concentrations of a test compound for 72 h at 37 °C in a humidified incubator with 5% CO_2. We determined the 50% growth inhibitory concentration (IC_{50}) using the CurveExpert 1.4 program. The mean values of three independent experiments were reported.

Semiquantitative RT-PCR Analysis. We grew the A549 cancer cells (3.0×10^5 cells) on a 6-well tissue culture plate for 24 h before they were treated with a test compound at 37 °C in a humidified CO_2 (5%) incubator for another 24 h. The mRNA was converted to cDNA using RevertAid reverse transcriptase (Thermo Scientific U.S.A.) and oligo-(dT)18 primer. We then amplified the cDNAs by PCR, and the products were separated by agarose gel electrophoresis. Supporting Information Table S6 summarizes the primer sequences, the annealing temperatures, the number of PCR cycles, and product sizes.

Telomerase Assay of Perylene-Treated Cancer Cells. We grew the A549 cancer cells (3.0×10^5 cells) on a 6-well tissue culture plate for 24 h before they were treated with a test compound at 37 °C in a humidified CO_2 (5%) incubator for another 48 h. CHAPS lysis buffer (50 μL) was then used to lyze the cells. We collected the supernatant and quantified the protein concentration using the Bradford assay (BioRad). This crude protein extract (8 μg) was used for each telomerase assay. The following TRAP assay was performed similarly to the cell-free telomerase assay above, except for using MTS primer (instead of TSG4) and without test compound extraction.

Statistical Analysis. We reported all statistic values as mean ± standard derivation (mean ± SD) from three independent experiments. The one-way analysis of variance (ANOVA) with Dunnett's test compared the treated groups and the controls. Differences are considered statistically significant when $*p < 0.05$, $**p < 0.01$, or $***p < 0.001$.

■ ASSOCIATED CONTENT

Supporting Information

The Supporting Information is available free of charge at https://pubs.acs.org/doi/10.1021/acsomega.2c01343.

Synthesis and characterization of perylene monoimide derivatives [^{1}H NMR (400 MHz) spectrum, MS data, and TLC]; hydrosolubility of PMIs and PIPER; visible light absorption and fluorescence emission spectra of the perylenes; predicted binding mode of PMIs and PIPER to two G4 DNAs by molecular docking; estimated binding affinity of PMIs and PIPER to two G4 DNAs (Table S1); suppression of *hTERT* expression (A) and telomerase activity (B) by PIPER in A549 lung cancer cells; the IC_{50} values (μM) of doxorubicin in various cells (Table S2); oligonucleotides used in the DNA binding study by spectrophotometry (Table S3); oligonucleotides used in the duplex−quadruplex competition assay (Table S4); oligonucleotides used in the modified fluorescent TRAP assay (Table S5); PCR-related information on the semiquantitative RT-PCR assay (Table S6) (PDF)

■ AUTHOR INFORMATION

Corresponding Authors

T. Randall Lee − *Department of Chemistry and the Texas Center for Superconductivity, University of Houston, Houston, Texas 77204-5003, United States;* orcid.org/0000-0001-9584-8861; Phone: +1-713-743-2724; Email: trlee@uh.edu

Wirote Tuntiwechapikul − *Department of Biochemistry, Faculty of Medicine, Chiang Mai University, Chiang Mai 50200, Thailand; Center for Research and Development of Natural Products for Health, Chiang Mai University, Chiang Mai 50200, Thailand;* orcid.org/0000-0003-1365-476X; Phone: +66-53-945323; Email: wirotetunti@yahoo.com

Authors

Pak Thaichana − *Department of Biochemistry, Faculty of Medicine, Chiang Mai University, Chiang Mai 50200, Thailand*

Ratasark Summart − *Department of Biochemistry, Faculty of Medicine, Chiang Mai University, Chiang Mai 50200, Thailand*

Pornngarm Dejkriengkraikul − *Department of Biochemistry, Faculty of Medicine, Chiang Mai University, Chiang Mai 50200, Thailand; Center for Research and Development of Natural Products for Health, Chiang Mai University, Chiang Mai 50200, Thailand*

Puttinan Meepowpan − *Department of Chemistry, Faculty of Science, Chiang Mai University, Chiang Mai 50200, Thailand*

Complete contact information is available at: https://pubs.acs.org/10.1021/acsomega.2c01343

Notes

The authors declare no competing financial interest.

■ ACKNOWLEDGMENTS

This research was funded by (a) the Thailand Research Fund (RSA5880007), (b) the Royal Golden Jubilee Ph.D. (RGJ-Ph.D.) Program (PHD/0198/2556 and PHD/0052/2557), (c) Faculty of Medicine, Chiang Mai University (045-2561 and 002-2565), (d) the Robert A. Welch Foundation (Grant E-1320), and (e) the Center for Research and Development of Natural Products for Health, Chiang Mai University, Thailand.

REFERENCES

(1) Hanahan, D.; Weinberg, R. A. Hallmarks of cancer: the next generation. *Cell.* **2011**, *144*, 646−674.
(2) Jafri, M. A.; Ansari, S. A.; Alqahtani, M. H.; Shay, J. W. Roles of telomeres and telomerase in cancer, and advances in telomerase-targeted therapies. *Genome Med.* **2016**, *8*, 69.
(3) Shay, J. W.; Wright, W. E. Telomeres and telomerase: three decades of progress. *Nat. Rev. Genet.* **2019**, *20*, 299−309.
(4) Brown, A. F.; Podlevsky, J. D.; Qi, X.; Chen, Y.; Xie, M.; Chen, J. J. A self-regulating template in human telomerase. *Proc. Natl. Acad. Sci. U. S. A.* **2014**, *111*, 11311−11316.
(5) Bhattacharyya, D.; Arachchilage, M. G.; Basu, S. Metal cations in G-quadruplex folding and stability. *Front. Chem.* **2016**, *4*, 38.
(6) Hansel-Hertsch, R.; Beraldi, D.; Lensing, S. V; Marsico, G.; Zyner, K.; Parry, A.; Di Antonio, M.; Pike, J.; Kimura, H.; Narita, M.; Tannahill, D.; Balasubramanian, S. G-quadruplex structures mark human regulatory chromatin. *Nat. Genet.* **2016**, *48*, 1267−1272.
(7) Varshney, D.; Spiegel, J.; Zyner, K.; Tannahill, D.; Balasubramanian, S. The regulation and functions of DNA and RNA G-quadruplexes. *Nat. Rev. Mol. Cell Biol.* **2020**, *21*, 459−474.
(8) Sanchez-Martin, V.; Lopez-Pujante, C.; Soriano-Rodriguez, M.; Garcia-Salcedo, J. A. An updated focus on quadruplex structures as potential therapeutic targets in cancer. *Int. J. Mol. Sci.* **2020**, *21*, 8900.
(9) Savva, L.; Georgiades, S. N. Recent developments in small-molecule ligands of medicinal relevance for harnessing the anticancer potential of G-quadruplexes. *Molecules.* **2021**, *26*, 841.
(10) Teng, F. Y.; Jiang, Z. Z.; Guo, M.; Tan, X. Z.; Chen, F.; Xi, X. G.; Xu, Y. G-quadruplex DNA: a novel target for drug design. *Cell. Mol. Life Sci.* **2021**, *78*, 6557−6583.
(11) Riou, J. F.; Guittat, L.; Mailliet, P.; Laoui, A.; Renou, E.; Petitgenet, O.; Mégnin-Chanet, F.; Hélène, C.; Mergny, J. L. Cell senescence and telomere shortening induced by a new series of specific G-quadruplex DNA ligands. *Proc. Natl. Acad. Sci. U. S. A.* **2002**, *99*, 2672−2677.
(12) Burger, A. M.; Dai, F.; Schultes, C. M.; Reszka, A. P.; Moore, M. J.; Double, J. A.; Neidle, S. The G-quadruplex-interactive molecule BRACO-19 inhibits tumor growth, consistent with telomere targeting and interference with telomerase function. *Cancer Res.* **2005**, *65*, 1489−1496.
(13) Neidle, S. Human telomeric G-quadruplex: the current status of telomeric G-quadruplexes as therapeutic targets in human cancer. *FEBS J.* **2010**, *277*, 1118−1125.
(14) Iachettini, S.; Stevens, M. F.; Frigerio, M.; Hummersone, M. G; Hutchinson, I.; Garner, T. P; Searle, M. S; Wilson, D. W; Munde, M.; Nanjunda, R.; D'Angelo, C.; Zizza, P.; Rizzo, A.; Cingolani, C.; De Cicco, F.; Porru, M.; D'Incalci, M.; Leonetti, C.; Biroccio, A.; Salvati, E. On and off-target effects of telomere uncapping G-quadruplex selective ligands based on pentacyclic acridinium salts. *J. Exp. Clin. Cancer Res.* **2013**, *32*, 68.
(15) Berei, J.; Eckburg, A.; Miliavski, E.; Anderson, A. D.; Miller, R. J.; Dein, J.; Giuffre, A. M.; Tang, D.; Deb, S.; Racherla, K. S.; Patel, M.; Vela, M. S.; Puri, N. Potential telomere-related pharmacological Targets. *Curr. Top. Med. Chem.* **2020**, *20*, 458−484.
(16) Seimiya, H. Crossroads of telomere biology and anticancer drug discovery. *Cancer Sci.* **2020**, *111*, 3089−3099.
(17) Neidle, S. Quadruplex nucleic acids as novel therapeutic targets. *J. Med. Chem.* **2016**, *59*, 5987−6011.
(18) Islam, M. K.; Jackson, P. J.; Rahman, K. M.; Thurston, D. E. Recent advances in targeting the telomeric G-quadruplex DNA sequence with small molecules as a strategy for anticancer therapies. *Future Med. Chem.* **2016**, *8*, 1259−1290.
(19) Palumbo, S. L.; Ebbinghaus, S. W.; Hurley, L. H. Formation of a unique end-to-end stacked pair of G-quadruplexes in the hTERT core promoter with implications for inhibition of telomerase by G-quadruplex-interactive ligands. *J. Am. Chem. Soc.* **2009**, *131*, 10878−10891.
(20) Taka, T.; Huang, L.; Wongnoppavich, A.; Tam-Chang, S. W.; Lee, T. R.; Tuntiwechapikul, W. Telomere shortening and cell senescence induced by perylene derivatives in A549 human lung cancer cells. *Bioorg. Med. Chem.* **2013**, *21*, 883−890.
(21) Micheli, E.; D'Ambrosio, D.; Franceschin, M.; Savino, M. Water soluble cationic perylene derivatives as possible telomerase inhibitors: the search for selective G-quadruplex targeting. *Mini-Rev. Med. Chem.* **2009**, *9*, 1622−1632.
(22) Kern, J. T.; Kerwin, S. M. The aggregation and G-quadruplex DNA selectivity of charged 3,4,9,10-perylenetetracarboxylic acid diimides. *Bioorg. Med. Chem. Lett.* **2002**, *12*, 3395−3398.
(23) Kaewtunjai, N.; Summart, R.; Wongnoppavich, A.; Lojanapiwat, B.; Lee, T. R.; Tuntiwechapikul, W. Telomerase inhibition, telomere shortening, and cellular uptake of the perylene derivatives PM2 and PIPER in prostate cancer cells. *Biol. Pharm. Bull.* **2019**, *42*, 906−914.
(24) Taka, T.; Joonlasak, K.; Huang, L.; Randall, L. T.; Chang, S. W.; Tuntiwechapikul, W. Down-regulation of the human VEGF gene expression by perylene monoimide derivatives. *Bioorg. Med. Chem. Lett.* **2012**, *22*, 518−522.
(25) Samudrala, R.; Zhang, X.; Wadkins, R. M.; Mattern, D. L. Synthesis of a non-cationic, water-soluble perylenetetracarboxylic diimide and its interactions with G-quadruplex-forming DNA. *Bioorg. Med. Chem.* **2007**, *15*, 186−193.
(26) Tuntiwechapikul, W.; Taka, T.; Béthencourt, M.; Makonkawkeyoon, L.; Randall, L. T. The influence of pH on the G-quadruplex binding selectivity of perylene derivatives. *Bioorg. Med. Chem. Lett.* **2006**, *16*, 4120−4126.
(27) Franceschin, M.; Pascucci, E.; Alvino, A.; D'Ambrosio, D.; Bianco, A.; Ortaggi, G.; Savino, M. New highly hydrosoluble and not self-aggregated perylene derivatives with three and four polar sidechains as G-quadruplex telomere targeting agents and telomerase inhibitors. *Bioorg. Med. Chem. Lett.* **2007**, *17*, 2515−2222.
(28) Summart, R.; Thaichana, P.; Supan, J.; Meepowpan, P.; Lee, T. R.; Tuntiwechapikul, W. Superiority of an asymmetric perylene diimide in terms of hydrosolubility, G-quadruplex binding, cellular uptake, and telomerase inhibition in prostate cancer cells. *ACS Omega.* **2020**, *5*, 29733−29745.
(29) Chen, S.; Xue, Z.; Gao, N.; Yang, X.; Zang, L. Perylene diimide-based fluorescent and colorimetric sensors for environmental detection. *Sensors (Basel).* **2020**, *20*, 917.
(30) Dey, S.; Sukul, P. K. Selective detection of pyrophosphate anions in aqueous medium using aggregation of perylene diimide as a fluorescent probe. *ACS Omega.* **2019**, *4*, 16191−16200.
(31) Huang, L.; Tam-Chang, S. W.; Seo, W.; Rove, K. Micro-fabrication of anisotropic organic materials via self-organization of an ionic perylenemonoimide. *Adv. Mater.* **2007**, *19*, 4149−4152.
(32) Huang, L.; Tam-Chang, S. W. 9-Piperazine substituted perylene-3,4-dicarboximide as a fluorescent probe in ratiometric analysis. *Chem. Commun.* **2011**, *47*, 2291−2293.
(33) Yan, C.; Barlow, S.; Wang, Z.; Yan, H.; Jen, A. K.-Y.; Marder, S. R.; Zhan, X. Non-fullerene acceptors for organic solar cells. *Nat. Rev. Mater.* **2018**, *3*, 18003.
(34) Luo, Y.; Yang, H.; Li, W.; Qin, Y. Construction of effective polymer solar cell using 1,7-disubstituted perylene diimide derivatives as electron transport layer. *ACS Omega.* **2019**, *4*, 21178−21186.
(35) Unnikrishnan, B.; Wu, R. S.; Wei, S. C.; Huang, C. C.; Chang, H. T. Fluorescent carbon dots for selective labeling of subcellular organelles. *ACS Omega.* **2020**, *5*, 11248−11261.
(36) Kern, J. T.; Thomas, P. W.; Kerwin, S. M. The relationship between ligand aggregation and G-quadruplex DNA selectivity in a series of 3,4,9,10-perylenetetracarboxylic acid diimides. *Biochemistry.* **2002**, *41*, 11379−11389.
(37) Franceschin, M.; Lombardo, C. M.; Pascucci, E.; D'Ambrosio, D.; Micheli, E.; Bianco, A.; Ortaggi, G.; Savino, M. The number and distances of positive charges of polyamine side chains in a series of perylene diimides significantly influence their ability to induce G-quadruplex structures and inhibit human telomerase. *Bioorg. Med. Chem.* **2008**, *16*, 2292−2304.

https://doi.org/10.1021/acsomega.2c01343
ACS Omega 2022, 7, 16746−16756

(38) Kalepu, S.; Nekkanti, V. Insoluble drug delivery strategies: review of recent advances and business prospects. *Acta. Pharm. Sin. B* **2015**, *5*, 442−453.
(39) Guryanov, I.; Naumenko, E.; Akhatova, F.; Lazzara, G.; Cavallaro, G.; Nigamatzyanova, L.; Fakhrullin, R. Selective Cytotoxic Activity of Prodigiosin@halloysite Nanoformulation. *Front. Bioeng. Biotechnol.* **2020**, *8*, 424.
(40) Vergara, D.; Bellomo, C.; Zhang, X.; Vergaro, V.; Tinelli, A.; Lorusso, V.; Rinaldi, R.; Lvov, Y. M.; Leporatti, S.; Maffia, M. Lapatinib/Paclitaxel polyelectrolyte nanocapsules for overcoming multidrug resistance in ovarian cancer. *Nanomedicine.* **2012**, *8*, 891−899.
(41) Soh, N.; Ueda, T. Perylene bisimide as a versatile fluorescent tool for environmental and biological analysis: a review. *Talanta.* **2011**, *85*, 1233−1237.
(42) Zhou, W.; Liu, G.; Yang, B.; Ji, Q.; Xiang, W.; He, H.; Xu, Z.; Qi, C.; Li, S.; Yang, S.; Xu, C. Review on application of perylene diimide (PDI)-based materials in environment: Pollutant detection and degradation. *Sci. Total Environ.* **2021**, *780*, 146483.
(43) Balasubramanian, S.; Neidle, S. G-quadruplex nucleic acids as therapeutic targets. *Curr. Opin. Chem. Biol.* **2009**, *13*, 345−353.
(44) Fedoroff, O. Y.; Salazar, M.; Han, H.; Chemeris, V. V.; Kerwin, S. M.; Hurley, L. H. NMR-Based model of a telomerase-inhibiting compound bound to G-quadruplex DNA. *Biochemistry.* **1998**, *37*, 12367−12374.
(45) Tuntiwechapikul, W.; Salazar, M. Cleavage of telomeric G-quadruplex DNA with perylene-EDTA*Fe(II). *Biochemistry* **2001**, *40*, 13652−13658.
(46) Monsen, R. C.; DeLeeuw, L.; Dean, W. L.; Gray, R. D.; Sabo, T. M.; Chakravarthy, S.; Chaires, J. B.; Trent, J. O. The hTERT core promoter forms three parallel G-quadruplexes. *Nucleic Acids Res.* **2020**, *48*, 5720−5734.
(47) Micheli, E.; Martufi, M.; Cacchione, S.; De Santis, P.; Savino, M. Self-organization of G-quadruplex structures in the hTERT core promoter stabilized by polyaminic side chain perylene derivatives. *Biophys. Chem.* **2010**, *153*, 43−53.
(48) Abdallah, P.; Luciano, P.; Runge, K. W.; Lisby, M.; Géli, V.; Gilson, E.; Teixeira, M. T. A two-step model for senescence triggered by a single critically short telomere. *Nat. Cell Biol.* **2009**, *11*, 988−993.
(49) Miyazaki, T.; Pan, Y.; Joshi, K.; Purohit, D.; Hu, B.; Demir, H.; Mazumder, S.; Okabe, S.; Yamori, T.; Viapiano, M.; Shin-ya, K.; Seimiya, H.; Nakano, I. Telomestatin impairs glioma stem cell survival and growth through the disruption of telomeric G-quadruplex and inhibition of the proto-oncogene, c-Myb. Clin. *Cancer Res.* **2012**, *18*, 1268−1280.
(50) Liu, W.; Sun, D.; Hurley, L. Binding of G-quadruplex-interactive agents to distinct G-quadruplexes induces different biological effects in MiaPaCa cells. *Nucleosides, nucleotides & nucleic acids.* **2005**, *24*, 1801−1815.
(51) Binz, N.; Shalaby, T.; Rivera, P.; Shin-ya, K.; Grotzer, M. A. Telomerase inhibition, telomere shortening, cell growth suppression and induction of apoptosis by telomestatin in childhood neuroblastoma cells. *Eur. J. Cancer.* **2005**, *41*, 2873−2881.
(52) Gowan, S. M.; Harrison, J. R.; Patterson, L.; Valenti, M.; Read, M. A.; Neidle, S.; Kelland, L. R. A G-quadruplex-interactive potent small-molecule inhibitor of telomerase exhibiting in vitro and in vivo antitumor activity. *Mol. Pharmacol.* **2002**, *61*, 1154−1162.
(53) Gunaratnam, M.; Greciano, O.; Martins, C.; Reszka, A. P.; Schultes, C. M.; Morjani, H.; Riou, J. F.; Neidle, S. Mechanism of acridine-based telomerase inhibition and telomere shortening. *Biochem. Pharmacol.* **2007**, *74*, 679−689.
(54) Incles, C. M.; Schultes, C. M.; Kempski, H.; Koehler, H.; Kelland, L. R.; Neidle, S. A G-quadruplex telomere targeting agent produces p16-associated senescence and chromosomal fusions in human prostate cancer cells. *Mol. Cancer. Ther.* **2004**, *10*, 1201−1206.
(55) Zhou, G.; Liu, X.; Li, Y.; Xu, S.; Ma, C.; Wu, X.; Cheng, Y.; Yu, Z.; Zhao, G.; Chen, Y. Telomere targeting with a novel G-quadruplex-interactive ligand BRACO-19 induces T-loop disassembly and telomerase displacement in human glioblastoma cells. *Oncotarget.* **2016**, *7*, 14925−14939.
(56) Vichai, V.; Kirtikara, K. Sulforhodamine B colorimetric assay for cytotoxicity screening. *Nat. Protoc.* **2006**, *1*, 1112−1116.

https://doi.org/10.1021/acsomega.2c01343
ACS Omega 2022, 7, 16746−16756